

Reduction of spectral phonon relaxation times from suspended to supported graphene

Bo Qiu and Xiulin Ruan^{a)}

School of Mechanical Engineering and the Birck Nanotechnology Center, Purdue University, West Lafayette, Indiana 47907-2088, USA

(Received 21 February 2012; accepted 19 April 2012; published online 7 May 2012)

We have performed molecular dynamics simulations with phonon spectral analysis to predict the mode-wise phonon relaxation times (RT) of suspended and supported graphene at room temperature, and the findings are consistent with recent optical measurements. For acoustic phonons, RTs reduce from up to 50 ps to less than 5 ps when graphene is put on silicon dioxide substrate. Similarly, optical phonon RTs reduce by half when supported. Stronger interfacial bonding is found to result in more RT reduction. Our results provide a fundamental understanding at the spectral phonon property level for the observed thermal conductivity reduction in supported graphene. © 2012 American Institute of Physics. [<http://dx.doi.org/10.1063/1.4712041>]

Ever since the experimental isolation in 2004,¹ graphene and its nanostructures have been the focus of extensive studies because of a number of fascinating properties they exhibit.²⁻⁶ Among them, the two-dimensional (2D) lattice structure and superior thermal conductivity make graphene particularly attractive for planar heat dissipation applications.^{4,7} Recent experiments found that the in-plane thermal conductivity of single-layer graphene (SLG) on a silicon dioxide (SiO₂) substrate was reduced from over 2500 W/m K (Refs. 4 and 8) to around 600 W/m K.⁹ As seen, substrates may limit the capability of in-plane thermal transport in supported SLG. A fundamental understanding of the decay channels and relaxation time (RT) of phonons in supported SLG will help identify the role of substrates and thereby facilitate the choice of substrate for high-performance graphene-based planar heat dissipation applications. Although substrate effects have been studied for some other nano-materials,^{10,11} no quantitative, adjustable parameter-free work on phonon scattering has been done to understand in-plane thermal transport in supported SLG. In this work, we employ molecular dynamics (MD) simulations in combination with spectral energy density (SED) analysis to extract spectral phonon RT for both suspended and supported SLG at room temperature. We find reduction in RTs of all phonon modes due to substrate scattering. We also find that stronger interfacial interactions will lead to further RT reduction. The predicted RT reduction is in line with the thermal conductivity reduction observed experimentally.⁹

In Fig. 1, we present the MD simulation domain setup for both suspended and supported SLG. The dimensions of the shown domains are $4.4 \times 4.3 \times 1.6 \text{ nm}^3$ for length, width, and height, respectively. Larger domain sizes are found to produce similar RTs for same phonon modes. Periodic boundary condition (PBC) is applied in the in-plane directions (parallel to graphene plane), while no restriction is applied to SLG vibration in the out-of-plane direction. We choose SiO₂ as the substrate to be consistent with recent experiments.⁹ A 2 nm thick block of amorphous SiO₂ which

comply with the PBC of the graphene domain is prepared by following the heating-quenching recipe used by Ong *et al.*¹² Similar thickness of substrate has been used previously for both electronic^{13,14} and thermal simulations.¹² Thicker SiO₂ block is not found to induce obvious difference in the in-plane thermal transport of supported graphene. To ensure stability and to approximate semi-infinite substrate, the bottom layer of amorphous SiO₂ is fixed. The graphene sheet is released from 2 Å above the substrate and allowed to conform to the SiO₂ surface freely. The geometries of both suspended and supported graphene are pre-optimized under constant pressure and temperature (NPT) for 6 ns to ensure zeroed pressure, equilibrated temperature, and stabilized interfacial structure before being used for individual simulation runs.

The LAMMPS package is used to perform all MD simulations.¹⁵ Optimized Tersoff (OPT) potentials¹⁶ are adopted to model C-C interactions in SLG. Interactions within SiO₂ are modeled using Tersoff potentials parameterized by Munetoh *et al.*¹⁷ C-Si and C-O interactions are assumed to be of van der Waals (vdW) type¹³ and modeled using Lennard-Jones (LJ) potentials

$$V(r_{ij}) = 4\epsilon \left[\left(\frac{\sigma}{r_{ij}} \right)^{12} - \left(\frac{\sigma}{r_{ij}} \right)^6 \right], \quad (1)$$

with parameters $\epsilon_{C-Si} = 8.909 \text{ meV}$, $\sigma_{C-Si} = 3.629 \text{ Å}$, $\epsilon_{C-O} = 3.442 \text{ meV}$, and $\sigma_{C-O} = 3.275 \text{ Å}$.¹⁸ The cutoff is chosen to be 2.7σ . Here r_{ij} is the separation between atom i and j . The timesteps for suspended and supported SLG simulations are chosen to be 0.8 and 0.2 fs, respectively, to ensure stability and resolution of all possible vibrational frequencies. Starting from pre-optimized geometries, after initial equilibration in constant volume and temperature ensemble (NVT), the systems are run in the constant volume and energy ensemble (NVE), from which the atomic velocities are extracted and post-processed. The phonon properties are found to converge for simulation lengths of 3.2 and 1.0 ns in NVE ensemble for suspended and supported SLG, respectively. In this work, only the thermal transport in x direction

^{a)}Electronic address: ruan@purdue.edu.

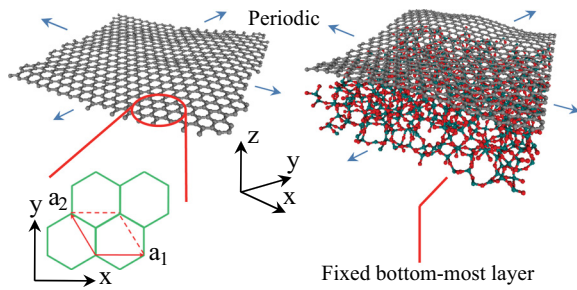


FIG. 1. Instantaneous geometry of both suspended and supported SLG. The SLG plane is parallel to the x - y plane while the SLG out-of-plane direction aligns with z .

(zig-zag) is considered. Five independent simulation runs are performed and averaged for each case study to minimize effects from statistical fluctuations. Since the temperatures at which we perform the MD simulations are below the Debye temperature of SLG (~ 1000 – 2300 K),¹⁹ temperature quantum corrections (QC) have been performed, which were practiced in similar ways in previous works.⁵ The phonon RT τ measures the temporal response of an activated phonon mode to return to equilibrium due to the net effect of different phonon scattering mechanisms. It can be defined as²⁰

$$\left(\frac{\partial f}{\partial t}\right)_{\text{collision}} = \frac{f - f_0}{\tau}, \quad (2)$$

where f is the phonon occupation number and f_0 is the equilibrium occupation number, which follows Bose-Einstein distribution. The SED method for phonon RT extraction from MD simulations has been used for a range of materials,^{21–25} and a similar method is used here. However, certain modifications are needed, and the details are presented in the supplemental material.²⁶

The per-branch phonon RTs for both suspended and supported SLG at 304 K as a function of wavevector \mathbf{k} and frequency are shown in Figs. 2(a) and 2(b), respectively. Because of symmetry, the phonon properties in the full Brillouin zone (BZ) can be reproduced by only studying the irreducible \mathbf{k} -space, which is 1/12th of the 1st BZ. However, because of the simplicity in discretization and specifying group velocity along x direction, we study the 1st quadrant of BZ instead. From Fig. 2(a), we indeed find the distribution of RTs in suspended SLG to be reasonably symmetrical about high symmetry lines, considering finite discretization and uncertainty in predicted RT values. This confirms the self-consistency of our approach. In addition, as seen in Fig. 2(a), the phonon dispersions in SLG with or without substrate do not differ much. Therefore, good correspondence between phonon modes in both cases can be well found to identify RT changes.

From Fig. 2, it is seen that, in suspended SLG, RT values of out-of-plane acoustic (ZA) phonons are in the range of sub 10–40 ps throughout BZ. The long RT of ZA phonons indicates relatively weak correlation between the in-plane and out-of-plane modes, which results in less scattering in ZA phonons.²⁷ It is interesting to see that out-of-plane optical (ZO) and ZA phonons have similarly large RTs, which can again be ascribed to the coupling strength between the in-plane and

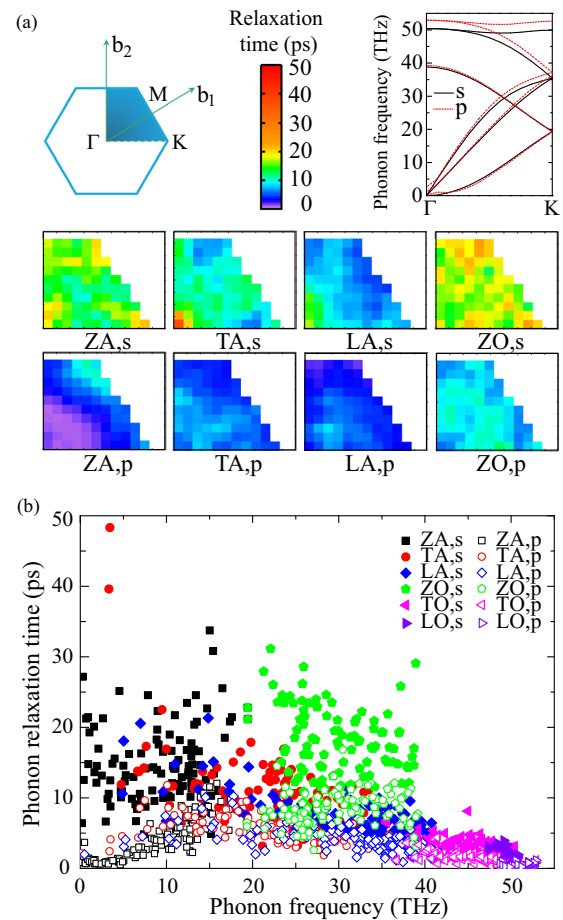


FIG. 2. (a) Distribution of phonon RT in the first quadrant of 1st BZ with the color representing RTs values. Also plotted are the phonon dispersions along Γ -K. (b) RT as a function of frequency for all phonon branches. The subscripts “s” and “p” are short for “suspended” and “supported”, respectively.

out-of-plane modes. The relatively weak dependence of ZA/ZO RT on the wavevector \mathbf{k} is also an indication that their coupling to in-plane phonons is not very strong. As frequency increases, RT of ZA phonons first decreases then increases as \mathbf{k} approaches BZ boundary. The relatively short RT of mid-frequency ZA phonons can be attributed to the fact that higher-order phonon scattering involving these modes is important and yields comparable scattering rates as that of three-phonon process, limiting the RT.²⁸

Away from the zone center, the overall RT is mainly around 20 ps and below in most regions of BZ for longitudinal acoustic (LA) and transverse acoustic (TA) phonons. As frequency increases, RT shortens due to more efficient Umklapp scattering. For LA and TA phonons near zone center with small frequencies, similar to ZA phonons, their RT tends to diverge as seen in Fig. 2(b). This is because these phonon modes have very small wavevectors that, due to the momentum and energy conservation requirements, barely scatter with other phonons.

When put on substrate, it is found that RTs are shortened throughout BZ and the full frequency range for all phonon branches. Namely, RTs of all acoustic phonons are generally shortened to be less than 10 ps. From the color map in Fig. 2(a), it can be clearly seen that such reduction is strongest for phonon modes closer to zone center. Also the distribution of RT in BZ becomes less symmetrical. This indicates the

introduction of substrate strongly destructs the long-range order of phonon transport through random scattering sites at the interface. From Fig. 2(b), it is seen that the RT of low frequency phonons are mostly shortened. For frequency below 18 THz, the RT values monotonically decrease as frequency continuously reduces to zero, indicating the substrate couples most efficiently to low frequency acoustic phonons. One of the most significant implication of such observation is that the thermal conductivity of supported graphene will not be sensitive to graphene flake size. This is because long wavelength near-zone-center phonons in larger samples will have minimal RT due to substrate scattering and thus barely contribute to thermal transport.

The RT reduction is especially strong for ZA modes. This is due to the fact that the presence of the substrate breaks various symmetries (mirror-reflection, translational, etc.) in SLG and alters the out-of-plane vibrations of SLG by introducing SLG-substrate scattering which largely shortens the RT of ZA phonons. In this case, higher-order anharmonic interactions are no longer important. Similar arguments can also be made to explain the reduction of RT of ZO phonons.

Recent Brillouin scattering experiment on multilayer graphene supported on SiO₂/Si substrate²⁹ suggests the RT of near-zone-center LA/TA phonon is about 10–30 ps, which is shorter than that of suspended graphene, in line with our findings. In fact, due to the amorphous nature of silica, the coordinations of surface silicon/oxygen atoms cannot comply with the periodicity of SLG. As a result, the presence of the “irregularly” coordinated silicon/oxygen atoms at the interface will couple to the in-plane vibrations of carbon atoms as scattering centers and essentially hinder the in-plane phonons in SLG from transporting in a perfect 2D lattice. To sustain long RT and thus high thermal conductivity of SLG, a substrate with better lattice match to SLG should be pursued. Therefore, a supported double-layer graphene (DLG) or SLG supported on boron nitride (BN) substrate may turn out to be better for planar heat dissipation applications.³⁰

The majority of longitudinal optical (LO) and transverse optical (TO) phonons are found to have RTs about 1–4 ps at room temperature and reduced by about half when put on substrate. This is consistent with the optical phonon RTs of supported few-layer graphene measured by Raman spectroscopy.^{31–33}

The calculated phonon RT is due to both Umklapp and normal scattering which cannot be separated in the current approach. As pointed out in Ref. 27, normal scattering could be an important scattering channel in graphene, so it may not be appropriate to use these RTs in the Callway-Holland approach³⁴ to calculate the thermal conductivity. However, the reduced phonon RTs provide a parameter-free understanding of the thermal conductivity reduction in supported graphene at the mode-wise phonon level.

The above results for supported SLG are obtained under the assumption that the interfacial interactions between SLG and substrate is of vdW type.¹³ On the other hand, it is found that covalent bonds can form between graphene and SiC substrate.³⁵ To explore the effects of interfacial bondings on the thermal transport in supported SLG, we study (a) RTs when LJ interactions are assumed to be 10 times stronger than

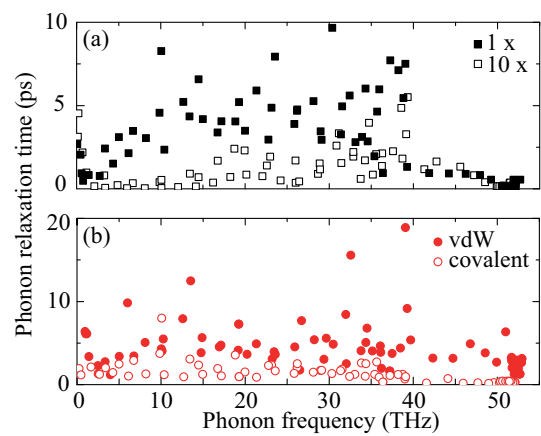


FIG. 3. RT of all phonon branches along $\Gamma - K$ in supported SLG. (a) SiO₂ substrate, when 10 times stronger LJ interactions assumed. (b) Silicon substrate, when covalent interfacial interactions are assumed.

used in previous sections and (b) RTs of graphene on silicon substrate with either vdW interactions or covalent bonds at the interface. For the latter case, we use LJ potentials with parameters $\epsilon_{C-Si} = 8.909$ meV, $\sigma_{C-Si} = 3.629$ Å to model vdW interactions while use OPT with mixing rules to model the C-Si covalent bonds. SED analysis is performed and the results are compared in $\Gamma - K$ direction, as shown in Figs. 3(a) and 3(b). As seen, when the vdW interactions are 10 times stronger or all bonds at the interface are covalent, the phonon scattering in SLG due to substrate is stronger, leading to significantly shortened RT. Therefore, we hypothesize that the interaction strength and geometry at SLG-substrate interface should be deterministic factors for phonon RT reduction in supported SLG. Our theory is supported by recent experiment that polymeric residue can bring the thermal conductivity of suspended DLG down to around 600 W/mK,³⁶ which is similar to that found in SLG supported on SiO₂ substrate.⁹

In conclusion, we predict the phonon RT of both suspended and supported SLG using MD simulations and SED analysis. Our results are consistent with various phonon RT measurements of SLG. When put on SiO₂ substrate, RTs of all phonon branches are reduced, owing to the SLG-substrate scattering and the breakdown of symmetries in both in-plane and out-of-plane phonons. We suggest to use substrates with closer lattice match and weaker interaction to SLG for better planar heat dissipations.

This work is supported by the Air Force Office of Scientific Research (AFOSR) through the Discovery Challenge Thrust (DCT) Program (grant FA9550-11-1-0057, Program Manager Joan Fuller) and by the Cooling Technologies Research Center (CTRC), an NSF University/Industry Cooperation Research Center. We thank Alexander A. Balandin, Alan J. H. McGaughey, Jayathi Murthy, Asegun Henry, Joseph E. Turney, and Dhruv Singh for helpful discussions.

¹K. S. Novoselov, A. K. Geim, S. V. Morozov, D. Jiang, Y. Zhang, S. V. Dubonos, I. V. Grigorieva, and A. A. Firsov, *Science* **306**, 666 (2004).

²K. I. Bolotin, K. J. Sikes, Z. Jiang, M. Klim, G. Fudenberg, J. Hone, P. Kim, and H. L. Stormer, *Solid State Commun.* **146**, 351 (2008).

³C. Lee, X. Wei, J. W. Kysar, and J. Hone, *Science* **321**, 385 (2008).

- ⁴A. A. Balandin, S. Ghosh, W. Bao, I. Calizo, D. Teweldebrhan, F. Miao, and C. N. Lau, *Nano Lett.* **8**, 902 (2008).
- ⁵J. Hu, X. Ruan, and Y. P. Chen, *Nano Lett.* **9**, 2730 (2009).
- ⁶Y. Wang, S. Chen, and X. Ruan, *Appl. Phys. Lett.* **100**, 163101 (2012).
- ⁷A. A. Balandin, *Nature Mater.* **10**, 569 (2011).
- ⁸W. Cai, A. L. Moore, Y. Zhu, X. Li, S. Chen, L. Shi, and R. S. Ruoff, *Nano Lett.* **10**, 1645 (2010).
- ⁹J. H. Seol, I. Jo, A. L. Moore, L. Lindsay, Z. H. Aitken, M. T. Pettes, X. Li, Z. Yao, R. Huang, D. Broido *et al.*, *Science* **328**, 213 (2010).
- ¹⁰A. V. Savin, B. Hu, and Y. S. Kivshar, *Phys. Rev. B* **80**, 195423 (2009).
- ¹¹Z.-Y. Ong, E. Pop, and J. Shiomi, *Phys. Rev. B* **84**, 165418 (2011).
- ¹²Z.-Y. Ong and E. Pop, *Phys. Rev. B* **81**, 155408 (2010).
- ¹³R. H. Miwa, W. Orellana, and A. Fazzio, *Appl. Surf. Sci.* **244**, 124 (2005).
- ¹⁴A. K. Vallabhaneni, B. Qiu, J. Hu, Y. P. Chen, and X. Ruan, "Interfacial thermal conductance of vertical graphene nanoribbon on a silicon substrate" (unpublished).
- ¹⁵S. Plimpton, *J. Comput. Phys.* **117**, 1 (1995).
- ¹⁶L. Lindsay and D. A. Broido, *Phys. Rev. B* **81**, 205441 (2010).
- ¹⁷S. Munetoh, T. Motooka, K. Moriguchi, and A. Shintani, *Comput. Mater. Sci.* **39**, 334 (2007).
- ¹⁸A. K. Rappe, C. J. Casewit, K. S. Colwell, W. A. Goddard, and W. M. Skiff, *J. Am. Chem. Soc.* **114**, 10024 (1992).
- ¹⁹V. K. Tewary and B. Yang, *Phys. Rev. B* **79**, 125416 (2009).
- ²⁰J. M. Ziman, *Electrons and Phonons* (Oxford University Press, London, 1960).
- ²¹N. de Koker, *Phys. Rev. Lett.* **103**, 125902 (2009).
- ²²J. A. Thomas, J. E. Turney, R. M. Iutzi, C. H. Amon, and A. J. H. McGaughey, *Phys. Rev. B* **81**, 081411 (2010).
- ²³B. Qiu, H. Bao, G. Zhang, Y. Wu, and X. Ruan, *Comput. Mater. Sci.* **53**, 278 (2012).
- ²⁴B. Qiu, Y. Wang, and X. Ruan, Proceedings of MRS Spring Meeting, 2011, MRSS11-1347-BB10-08, San Francisco, CA, USA.
- ²⁵B. Qiu and X. Ruan, Proceedings of ASME IMECE 2011, IMECE2011-62963, Denver, CO, USA.
- ²⁶See supplementary material at <http://dx.doi.org/10.1063/1.4712041> for the details of RT extraction using SED method.
- ²⁷L. Lindsay, D. A. Broido, and N. Mingo, *Phys. Rev. B* **82**, 115427 (2010).
- ²⁸N. W. Ashcroft and N. D. Mermin, *Solid State Physics* (Brooks Cole, 1976).
- ²⁹Z. K. Wang, H. S. Lim, S. C. Ng, B. Ozyilmaz, and M. H. Kuok, *Carbon* **46**, 2133 (2008).
- ³⁰Z. Wang, R. Xie, C. T. Bui, D. Liu, X. Ni, B. Li, and J. T. L. Thong, *Nano Lett.* **11**, 113 (2011).
- ³¹K. Kang, D. Abdula, D. G. Cahill, and M. Shim, *Phys. Rev. B* **81**, 165405 (2010).
- ³²H. Wang, J. H. Strait, P. A. George, S. Shivaraman, V. B. Shields, M. Chandrashekar, J. Hwang, F. Rana, M. G. Spencer, C. S. Ruiz-Vargas *et al.*, *Appl. Phys. Lett.* **96**, 081917 (2010).
- ³³I. Calizo, W. Bao, F. Miao, C. N. Lau, and A. A. Balandin, *Appl. Phys. Lett.* **91**, 201904 (2007).
- ³⁴M. G. Holland, *Phys. Rev.* **132**, 2461 (1963).
- ³⁵A. Mattausch and O. Pankratov, *Phys. Rev. Lett.* **99**, 076802 (2007).
- ³⁶M. T. Pettes, I. Jo, Z. Yao, and L. Shi, *Nano Lett.* **11**, 1195 (2011).